

A GRADIENT BASED OPTIMIZATION FRAMEWORK FOR THE DESIGN OF SINGLE AND MULTI-STAGE METAL FORMING PROCESSES

Akkaram Srikanth and Nicholas Zabaras

Sibley School of Mechanical and Aerospace Engineering
188 Frank H. T. Rhodes Hall, Cornell University
Ithaca, NY 14853-3801
Email : zabaras@cornell.edu

ABSTRACT A gradient based optimization methodology is developed for the design of metal forming processes. A novel, efficient and mathematically rigorous scheme is developed for a continuum based sensitivity analysis of metal forming processes that is used to accurately evaluate gradients of the objective function and design constraints. In particular, a sensitivity analysis is developed for the Lagrangian analysis of finite inelastic deformations of hyperelastic-viscoplastic materials involving frictional contact. A framework for shape as well as parameter optimization for single-stage metal forming processes is developed [1], [2]. Weak sensitivity equilibrium equations are derived for the large deformation of the workpiece in a typical forming operation. This sensitivity kinematic problem is linearly coupled with the appropriate sensitivity constitutive and contact sub-problems. Thus a linear sensitivity problem with appropriate driving forces is identified and the analysis carried out in an infinite dimensional framework. This work on the design of single-stage forming processes is currently expanded to include the design of multi-stage forming processes which necessarily involve the computation of both shape as well as non-shape (parameter) sensitivities. The direct deformation and sensitivity deformation problems are implemented using the finite element method. The effectiveness of the proposed methodology is demonstrated by solving a couple of practical design problems in single as well as multi-stage forming processes.

INTRODUCTION The primary objective of a metal forming process sequence is to efficiently induce a desired shape change on a billet while maintaining desired material property levels in the final product. Accurate prediction of large deformations, nature of the microstructural changes in polycrystalline metals, contact and friction conditions at the workpiece-die interface are few of the challenges that one must consider while developing means for the design and analysis of metal forming processes. Desired objectives in a single stage forming operation may include one or more of

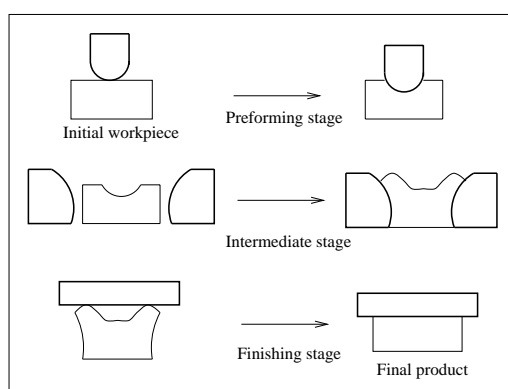


FIGURE 1: Schematic of a multi-stage forging sequence depicting the process of uniformly increasing the cross section of an initial round bar stock.

the following criteria: (a) uniform deformation in the final product (b) minimum work spent in deforming the material (c) desired microstructure in the final product (d) desired shape of the final product etc. These objectives can be satisfied by controlling design variables that can represent the initial shape of the workpiece, shape of the die, process parameters like lubrication conditions at the die-workpiece interface, thermal boundary conditions etc. In most industrial forming applications, the desired objectives indicated above are seldom simple enough to be achieved in a single forming operation. As a result, intermediate deformation or preforming steps are used to efficiently transform the initial geometry into a final shape and/or with desired material properties. Thermal processing is also used in between deformation stages to control the microstructure or product quality. A schematic of a simple forging sequence depicting the process of uniformly increasing the cross section of an initial round bar stock is shown in Fig. 1.

Optimization of multi-stage processes may be viewed as the design of the forming sequence, that converts the initial workpiece to the final product while meeting the desired manufacturing objectives and satisfying various process constraints. A forming sequence can be viewed at two levels for the purpose of optimization (a) the broad identification of the number, type and order of forming/heat-treatment operations that make up the sequence (e.g forward extrusion, open die forging etc.) and (b) the specific identification/selection of design variables in each of the forming operations (e.g ram speed in extrusion, die shape or stroke in a preforming stage etc.). In the present work, the identification of the forming operations is assumed a priori known and the focus is on making design decisions at the second level in a robust, efficient and automatic manner. In particular, a gradient based approach is used to solve the multi-stage optimization problem and this necessitates the evaluation of the gradient of the objective function and/or process constraints with respect to the design variables in each of the forming operations that constitute the sequence. Sensitivity analysis is a method which is widely used to evaluate design gradients. In this paper, we develop a generic scheme to compute the sensitivities of single stage as well as multi-stage forming processes (Fig. 2). Sensitivities or design sensitivities of the deformation or material state are quantitative measures of changes in the deformation and material state, respectively, as a result of perturbations to the design variables. Sensitivity analysis of a multi-stage process necessarily involves the computation of both shape as well as parameter sensitivities. However, unlike single stage shape sensitivity analysis where the initial workpiece shape depends explicitly on shape design variables, the intermediate preform shape in a generic forming stage of a multi-stage process depends implicitly on the design variables (non-shape parameters) that define the processing history of the intermediate preform.

ANALYSIS OF THE FORMING SEQUENCE The solution of the direct deformation forming sequence involves computation of the time history of deformation as well as material state of a body deforming as a result of contact and friction at the die-workpiece interface in each of the forming operations that make up the sequence. An updated Lagrangian FEM formulation is used to solve the direct deformation problem in a generic forming stage in which material occupying an initial configuration (intermediate preform) B_o ($t = t_o$) is deformed to obtain a final configuration (final preform) B_f ($t = t_f$). In describing the deformation, field variables are monitored that occupied location \mathbf{X} in the intermediate preform and occupies a location $\mathbf{x} = \hat{\mathbf{x}}(\mathbf{X}, t)$, $t \in [t_o, t_f]$ in the deformed configuration. A material point at a location \mathbf{Y} in B_i occupies a position \mathbf{X} in B_o as a result

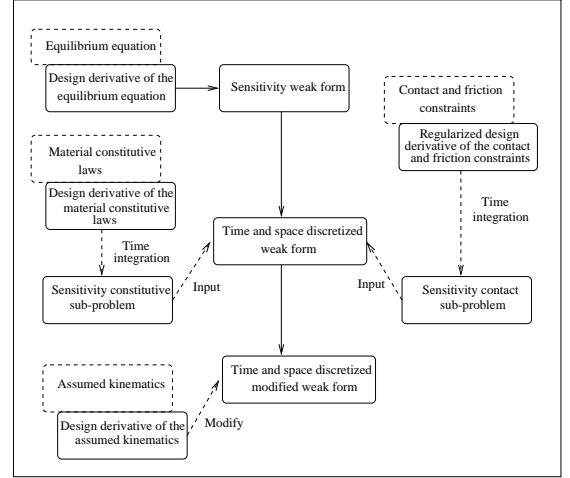


FIGURE 2: Schematic of the continuum sensitivity algorithm in a generic forming stage.

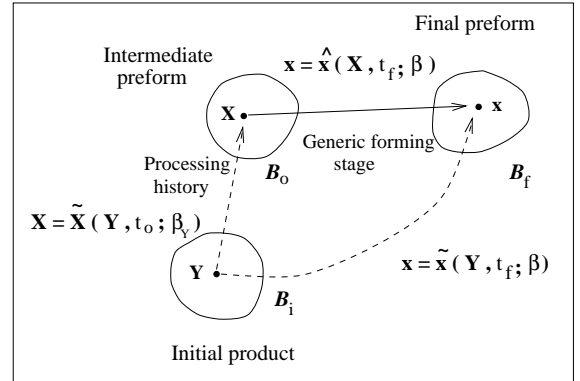


FIGURE 3: Schematic of a generic forming stage

of the deformation history. A schematic of a generic forming stage is represented in Fig. 3, along with the virgin product. The total deformation gradient \mathbf{F} , with respect to the virgin configuration B_i is assumed to be decomposed as :

$$\mathbf{F} = \nabla_{\mathbf{Y}} \tilde{\mathbf{x}}(\mathbf{Y}, t) = \frac{\partial \tilde{\mathbf{x}}(\mathbf{Y}, t)}{\partial \mathbf{Y}} = \mathbf{F}^e \mathbf{F}^p \quad (1)$$

where \mathbf{F}^e is the elastic deformation gradient and \mathbf{F}^p is the plastic deformation gradient. The equilibrium equations can be expressed in the intermediate preform configuration B_o as

$$\nabla_{\mathbf{X}} \cdot \mathbf{P} + \mathbf{f} = 0 \quad (2)$$

where the Piola-Kirchhoff I stress $\mathbf{P}(\mathbf{X}, t)$ is expressed

as

$$\mathbf{P}(\mathbf{X}, t) = \det \mathbf{F}_r \mathbf{T} \mathbf{F}_r^{-T} \quad (3)$$

and \mathbf{f} refers to the referential body force density. \mathbf{T} represents the Cauchy stress and $\mathbf{F}_r = \mathbf{F}(\mathbf{F}_o)^{-1}$ is the relative deformation gradient with respect to the intermediate preform \mathbf{B}_o . Here \mathbf{F}_o refers to the deformation gradient of the intermediate preform with respect to the virgin product i.e. $\nabla_Y \mathbf{X}$.

In order to solve the equilibrium equations, the constitutive relationship between the Cauchy stress \mathbf{T} and the deformation gradient \mathbf{F} should be specified. Following Anand *et al.* [4], the hyperelastic-viscoplastic constitutive equations are summarized here:

$$\begin{aligned} \mathbf{F}^e &= \mathbf{R}^e \mathbf{U}^e \\ \bar{\mathbf{T}} &= \mathcal{L}^e [\ln \mathbf{U}^e] \\ \bar{\mathbf{D}}^p &= \dot{\mathbf{F}}^p (\mathbf{F}^p)^{-1} = \frac{3}{2} \frac{\dot{\tilde{\epsilon}}^p \bar{\mathbf{T}}'}{\tilde{\sigma}} \\ \tilde{\sigma} &= \sqrt{\frac{3}{2} \bar{\mathbf{T}}' \cdot \bar{\mathbf{T}}'} \\ \dot{\tilde{\epsilon}}^p &= f(\tilde{\sigma}, s) \\ \dot{s} &= g(\tilde{\sigma}, s) \end{aligned} \quad (4)$$

where $\mathbf{R}^e, \mathbf{U}^e$ are computed from the polar decomposition of \mathbf{F}^e , $\bar{\mathbf{T}}$ is the pullback of the Kirchhoff stress with respect to \mathbf{R}^e , $\bar{\mathbf{T}}'$ is the deviatoric part of $\bar{\mathbf{T}}$, $\tilde{\sigma}$ is the equivalent stress, $\tilde{\epsilon}^p$ is the equivalent plastic strain and s is the isothermal scalar resistance to deformation.

Contact and friction is modeled following the scheme suggested by Simo and Laursen in [5]. A schematic of the contact problem is shown in Fig. 4. The die \mathcal{D} is parametrized in two dimensions using a parameter ξ and the function $\mathbf{y}(\xi)$, $0 \leq \xi \leq 1$. We introduce a fixed right-handed basis $(\mathbf{e}_1, \mathbf{e}_2, \mathbf{e}_3)$ and a convected basis $(\mathbf{r}, \mathbf{e}_2, \boldsymbol{\nu})$ at each point defined by a particular value of ξ . The tangent vector $\boldsymbol{\tau}_1$ and the unit tangent vector \mathbf{r} are given by

$$\boldsymbol{\tau}_1 = \mathbf{y}_{,\xi} \quad \mathbf{r} = \frac{\boldsymbol{\tau}_1}{\|\boldsymbol{\tau}_1\|} \quad (5)$$

The die separates the space into admissible and inadmissible regions and $\Gamma \subset \partial \mathbf{B}_o$ refers to the part of the boundary that could potentially come in contact. We define the gap function g of any point \mathbf{x} in space as the shortest distance of that point from the die:

$$\bar{\mathbf{y}} - \mathbf{x} = g(\mathbf{x}) \boldsymbol{\nu}(\bar{\mathbf{y}}) \quad (6)$$

where $\bar{\mathbf{y}} \in \mathcal{D}$ is the value of \mathbf{y} that minimizes the norm $\|\mathbf{x} - \mathbf{y}\|$. With this definition of the gap function, the impenetrability constraints are given as follows: For all

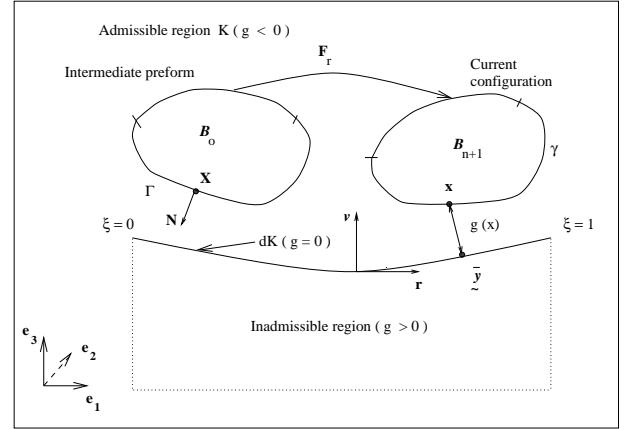


FIGURE 4: A schematic of the contact sub-problem in a generic forming stage showing the definition of the gap function, of the admissible and inadmissible regions.

$$\mathbf{X} \in \Gamma, \text{ with } \mathbf{x}_{n+1} = \hat{\mathbf{x}}(\mathbf{X}, t_{n+1})$$

$$\begin{aligned} g(\mathbf{x}_{n+1}) &\leq 0 \\ \lambda_N &= \boldsymbol{\nu} \cdot \boldsymbol{\lambda} \\ \lambda_N g(\mathbf{x}_{n+1}) &= 0 \end{aligned} \quad (7)$$

where λ_N is the absolute value of the contact pressure. The vector $\boldsymbol{\lambda}$ is the current traction per unit area in $\partial \mathbf{B}_o$. The Coulomb friction law can be written as:

$$\begin{aligned} \boldsymbol{\lambda}_T &= -\boldsymbol{\lambda} + \lambda_N \boldsymbol{\nu} \\ \Upsilon := \|\boldsymbol{\lambda}_T\| - \mu \lambda_N &\leq 0 \\ \mathbf{v}_T &= \chi \frac{\boldsymbol{\lambda}_T}{\|\boldsymbol{\lambda}_T\|} \\ \chi &\geq 0 \\ \chi \Upsilon &= 0 \end{aligned} \quad (8)$$

The solution of a generic stage in a forming sequence involves the solution to the principle of virtual work given as: Calculate $\hat{\mathbf{x}}(\mathbf{X}, t)$ such that:

$$\int_{\mathbf{B}_o} \mathbf{P}(\mathbf{F}_r) \cdot \nabla_X \tilde{\mathbf{u}} dV_o = \int_{\Gamma} \boldsymbol{\lambda} \cdot \tilde{\mathbf{u}} dA_o + \int_{\mathbf{B}_o} \mathbf{f} \cdot \tilde{\mathbf{u}} dV_o \quad (9)$$

for every admissible test function $\tilde{\mathbf{u}}$. The weak form is solved in an incremental-iterative manner as a result of material as well as geometric non-linearities.

The FEM is used for the solution of the weak form and the standard bi-linear quadrilateral with four Gauss integration points (full integration) performs poorly in the incompressible limit exhibiting an excessively stiff locking response. Moran *et al.* extended the \mathbf{B} -bar

method originally proposed by Hughes, to finite deformations [6]. The deformation gradient \mathbf{F} was multiplicatively decomposed into volumetric and deviatoric parts and a subsequent assumption in the treatment of the volumetric part was used in the discretized internal virtual work term. A reduced integration scheme was used in the treatment of the volumetric term and this introduced oscillations (hour-glass modes) in the solution. An a priori stabilization procedure using a scalar parameter was proposed to avoid these modes. de Souza Neto *et al.* proposed the \mathbf{F} -bar method which also uses the notion of the volumetric-deviatoric decomposition of \mathbf{F} [7]. The method differs from the \mathbf{B} -bar method in that, the assumption on the treatment of the volumetric part was only used in the constitutive relationship rather than in the internal virtual work. The \mathbf{F} -bar method with an a priori stabilization factor has been shown to work well for the current applications.

The continuum (compatible) deformation gradient \mathbf{F}_r with respect to the reference configuration \mathbf{B}_o admits the volumetric-deviatoric decomposition:

$$\begin{aligned}\mathbf{F}_r &= \mathbf{F}^{vol} \mathbf{F}^{dev} \\ \mathbf{F}^{vol} &= J^{\frac{1}{3}} \mathbf{I} \\ \mathbf{F}^{dev} &= J^{-\frac{1}{3}} \mathbf{F} \\ J &= \det(\mathbf{F})\end{aligned}\quad (10)$$

In the context of the finite element method, a discrete representation of \mathbf{F}_r i.e. $\bar{\mathbf{F}}_h$ in a typical finite element is defined as:

$$\begin{aligned}\bar{\mathbf{F}}_h &= \bar{\mathbf{F}}_h^{vol} \mathbf{F}_h^{dev} \\ \bar{\mathbf{F}}_h^{vol} &= \bar{J}_h^{\frac{1}{3}} \mathbf{I} = \left[\sum_{a=1}^{\overline{NINT}} J_{ha}(\bar{\xi}_a) \bar{N}_a \right]^{\frac{1}{3}} \mathbf{I} \\ \mathbf{F}_h^{dev} &= J_h^{-\frac{1}{3}} \mathbf{F}_h\end{aligned}\quad (11)$$

where $\bar{\xi}_a$, $a = 1, \dots, \overline{NINT}$ represent the reduced quadrature points and \bar{N}_a are the extrapolation (bar) shape functions such that $\bar{N}_a(\bar{\xi}_b) = \delta_{ab}$. A schematic of this decomposition is shown in Fig. 5. The use of a pre-determined number of volumetric degrees of freedom circumvents the issue of locking in nearly-incompressible deformations. However, the reduced integration leads to hour-glass instabilities in the deformation pattern [8]. In order to obtain a stable solution, an a priori stabilization method which introduces an empirical (small, positive) scalar parameter $\epsilon \rightarrow 0$, is used to define the assumed deformation gradient as

$$\mathbf{F}_h^{ave} \equiv \epsilon \mathbf{F}_h + (1 - \epsilon) \bar{\mathbf{F}}_h \quad (12)$$

In the \mathbf{F} -bar method, only the constitutive response is modified. Thus $\mathbf{P} \equiv \mathbf{P}(\mathbf{F}_h^{ave})$ is used in the finite

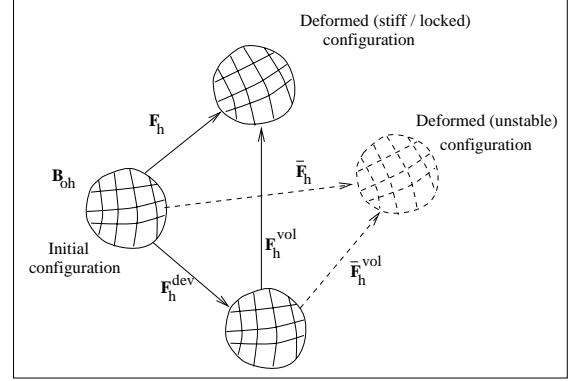


FIGURE 5: A schematic of the volumetric-deviatoric multiplicative decomposition used in the finite element model of the deformation

element representation of the internal work term i.e

$$\mathcal{G}_h^{int} \equiv \sum_e \int_{\Omega_e} \mathbf{P}(\mathbf{F}_h^{ave}) \cdot \nabla_X \tilde{\mathbf{u}}_h dV_o \quad (13)$$

Let us now consider the mechanics in-between two forming stages. This phase usually consists of an unloading process where one of the dies is removed from contact with the workpiece. The unloading process is elastic and as a result there is no evolution of the intermediate relaxed (unstressed) configuration and the isotropic scalar internal variable s . The unloading process is therefore modeled as a non-linear (finite deformation) elasto-static boundary value problem. If \mathbf{B} represents the final configuration of the workpiece at the end of the loading phase with the total deformation gradient given as $\mathbf{F} = \mathbf{F}^e \mathbf{F}^p$, then the solution to the unloading process results in the final body configuration \mathbf{B}_u with the total deformation gradient given as $\mathbf{F}_u = \mathbf{F}_u^e \mathbf{F}^p$. The modeling of the unloading phase (residual stresses) can be quite significant in the design of forgings with thin sections where residual stresses cause significant warpage. The workpiece material also undergoes a recovery process, whereby the material state evolves in the absence of an applied stress. The duration in-between forming stages is therefore characterized by the evolution of the inelastic internal variable s .

SENSITIVITY FIELDS In this section, we introduce notions of the sensitivity of various physical fields with respect to small changes in the design variables of the forming sequence given in Fig. 3. The deformation history leading to the intermediate preform which defines \mathbf{B}_o is described as follows:

$$\mathbf{X} = \tilde{\mathbf{X}}(\mathbf{Y}, t_o; \beta_Y), \quad \forall \mathbf{Y} \in \mathbf{B}_i \quad (14)$$

where β_Y represents the collection of design variables in all previous forming stages. The deformation in a generic (current) forming stage can be then represented as:

$$\mathbf{x} = \hat{\mathbf{x}}(\mathbf{X}, t; \beta), \quad \forall \mathbf{X} \in \mathbf{B}_o, \quad t \in (t_o, t_f) \quad (15)$$

where $\beta = \beta_X \cup \beta_Y$ and β_X represents the (non-shape) design variables in the current forming stage.

Consider the dependence of Lagrangian fields $\Phi = \hat{\Phi}(\mathbf{X}, t)$ on β . This dependence can be expressed as follows

$$\Phi = \hat{\Phi}(\tilde{\mathbf{X}}(\mathbf{Y}, t_o; \beta_Y), t; \beta) = \tilde{\Phi}(\mathbf{Y}, t; \beta) \quad (16)$$

The explicit dependence of Lagrangian fields on β_X i.e. $\Phi = \hat{\Phi}(\cdot, \cdot; \beta_X)$ reflects the unknown dependence of the fields on the non-shape design parameters of the current stage and can be treated in an analogous manner as in single stage forming processes. The explicit dependence of Lagrangian fields on β_Y i.e. $\Phi = \hat{\Phi}(\cdot, \cdot; \beta_Y)$ reflects the unknown dependence of the fields on the design parameters of previous forming stages. This dependence includes, for example (a) the variation of the current deformation as a result of changes in $Q = \tilde{Q}(\mathbf{Y}, t_o; \beta_Y)$ which represents a collection of variables (\mathbf{F}^p, s) that characterizes the intermediate preform \mathbf{B}_o (b) the variation in the contact history as a result of changes in the intermediate preform shape \mathbf{B}_o . These explicit dependencies are difficult to quantify directly. Lagrangian fields also depend implicitly on β_Y through the variable \mathbf{X} as a result of the deformation processing history.

The design differential $\overset{\circ}{\Phi}$ of a Lagrangian field is defined as the total Gateaux differential of $\Phi = \tilde{\Phi}(\mathbf{Y}, t; \beta)$ in the direction $\Delta\beta$ computed at β :

$$\begin{aligned} \overset{\circ}{\Phi} &\equiv \hat{\Phi}(\mathbf{X}, t; \beta, \Delta\beta) = \tilde{\Phi}(\mathbf{Y}, t; \beta, \Delta\beta) \\ &= \left. \frac{d}{d\lambda} \tilde{\Phi}(\mathbf{Y}, t; \beta + \lambda\Delta\beta) \right|_{\lambda=0} \end{aligned} \quad (17)$$

In the above equation β could represent either β_X or β_Y . The design differential or sensitivity $\overset{\circ}{\Phi}$ can be understood as representing the difference between two fields Φ , that result due to different designs defined by β and $\beta + \Delta\beta$ i.e.

$$\overset{\circ}{\Phi} = \tilde{\Phi}(\mathbf{Y}, t; \beta + \Delta\beta) - \tilde{\Phi}(\mathbf{Y}, t; \beta) + O(\|\Delta\beta\|^2) \quad (18)$$

It is emphasized that the fields $\tilde{\Phi}(\beta)$ and $\tilde{\Phi}(\beta + \Delta\beta)$ are computed for material points that occupy the same location \mathbf{Y} in the design independent virgin configuration \mathbf{B}_i . In the particular case where β represents the non-shape design parameters of the current forming stage

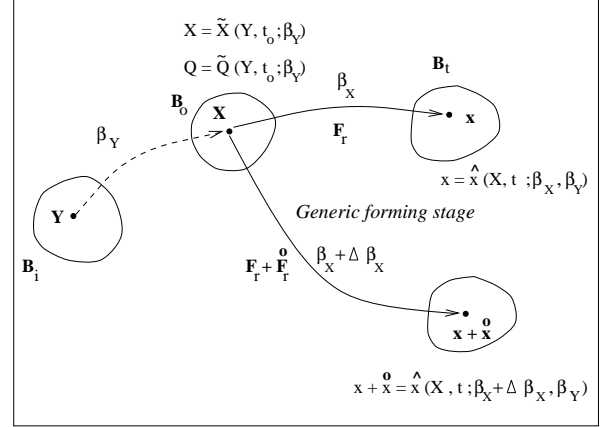


FIGURE 6: Schematic representation of the design sensitivity of the deformation in the current forming stage due to variations in the (non-shape) design parameters of current forming stage.

i.e. β_X , it is noted that equation (18) takes the usual form for the definition of parameter sensitivity:

$$\begin{aligned} \overset{\circ}{\Phi} &= \hat{\Phi}(\mathbf{X}, t; \beta_X + \Delta\beta_X, \beta_Y) - \\ &\hat{\Phi}(\mathbf{X}, t; \beta_X, \beta_Y) + O(\|\Delta\beta_X\|^2) \end{aligned} \quad (19)$$

The general representation in equation (18) allows for a unified treatment of shape as well as parameter sensitivity. The quantity $\overset{\circ}{\Phi}$ is of the same nature as Φ . A graphical representation of the notion of sensitivity due to variations in the design parameters β_X and β_Y are shown in Figures 6 and 7, respectively. In Fig. 7 the tensor $\mathbf{L}_\beta \equiv \nabla_{\mathbf{X}} \tilde{\mathbf{X}}(\mathbf{Y}, t_o; \beta_Y, \Delta\beta_Y) = \overset{\circ}{\mathbf{F}}_o \mathbf{F}_o^{-1}$ refers to the design velocity gradient. In the particular case of variations of the design parameter β_X , the design velocity gradient is $\mathbf{L}_\beta = \mathbf{0}$ (Fig. 6).

In order to provide insight on the notion of multi-stage sensitivity, we consider the following developments. Design sensitivities with respect to variations in the parameter β_X are treated in an analogous fashion as in single stage parameter sensitivity analysis. We therefore consider design sensitivity with respect to variations in the parameter β_Y here. Consider the dependence of $\hat{\Phi}(\mathbf{X}, t)$ on β_Y , this dependence results from the fact that the intermediate preform shape $\partial\mathbf{B}_o$ and state field distribution Q depend on β_Y . In particular we have :

$$\begin{aligned} \hat{\Phi}(\mathbf{X}, t; \beta_Y) &= \tilde{\Phi}(\mathbf{Y}, t; \beta_Y) \\ &= \tilde{\Phi}(\mathbf{Y}, t; \partial\mathbf{B}_o(\beta_Y), Q(\beta_Y)) \end{aligned} \quad (20)$$

Using equation (20) in equation (18), we can obtain

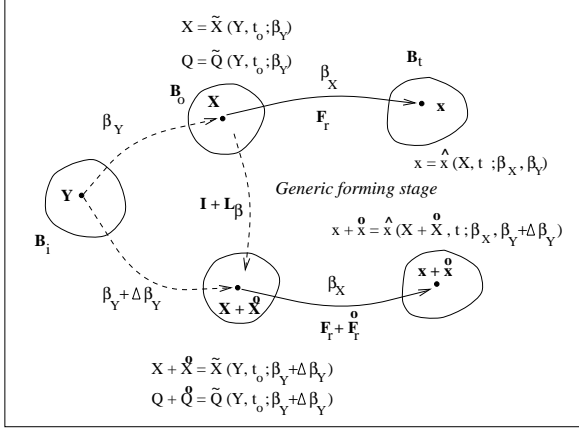


FIGURE 7: Schematic representation of the design sensitivity of the deformation in the current forming stage due to variations in the design parameters of previous forming stages.

that:

$$\begin{aligned} \overset{\circ}{\Phi} &= \frac{\partial \bar{\Phi}(\mathbf{Y}, t; \partial \mathbf{B}_o, Q)}{\partial (\partial \mathbf{B}_o)} \left[\frac{\partial (\partial \mathbf{B}_o)}{\partial \beta_Y} [\Delta \beta_Y] \right] \\ &+ \sum_i \frac{\partial \bar{\Phi}(\mathbf{Y}, t; \partial \mathbf{B}_o, Q)}{\partial Q_i} \left[\frac{\partial Q_i}{\partial \beta_Y} [\Delta \beta_Y] \right] \end{aligned} \quad (21)$$

To evaluate $\overset{\circ}{\Phi}$, one must first compute the Gateaux differentials of $\partial \mathbf{B}_o$ and Q with respect to a perturbation $\Delta \beta_Y$ in the design parameters of all previous forming stages. These Gateaux differentials, which define perturbations in the intermediate preform shape and state can be used to compute the Gateaux differential of Φ in the current forming stage. Thus, the computation of sensitivities for multi-stage processes must be performed in a sequential manner. The independent driving forces for the computation of sensitivities in the current forming stage are the design differentials of $\partial \mathbf{B}_o$ and Q . The recognition of the linear dependence of $\overset{\circ}{\Phi}$ on these design differentials (equation (21)) enables the efficient computation of design sensitivities of the current forming stage as demonstrated in the developments that follow.

SENSITIVITY WEAK FORM A weak form for the linear sensitivity analysis of a generic forming stage is identified by considering the sensitivity of the equilibrium equations and boundary conditions at the continuum level (Fig. 2). A unified weak form is developed to compute sensitivities with respect to any design parameter β . Appropriate features are then identified which contrast the sensitivity analysis performed with respect to β_X from β_Y . The sensitivity problem is posed using a

total Lagrangian formulation. The sensitivity deformation problem is developed on the intermediate preform \mathbf{B}_o . The design sensitivity of the equilibrium equation (2) results in:

$$\overline{\nabla_X \cdot \overset{\circ}{\mathbf{P}}} + \overset{\circ}{\mathbf{f}} = \mathbf{0}, \quad \forall \mathbf{X} \in \mathbf{B}_o, \quad \forall t \in [t_o, t_f] \quad (22)$$

A variational form for the sensitivity equilibrium equation can be posed as [1],[2]:

$$\begin{aligned} \int_{\mathbf{B}_o} \overset{\circ}{\mathbf{P}} \cdot \nabla_X \tilde{\boldsymbol{\eta}} dV_o - \int_{\mathbf{B}_o} \left(\overset{\circ}{\mathbf{P}} \left[\nabla_X \cdot \mathbf{L} \beta^T \right] \right) \cdot \tilde{\boldsymbol{\eta}} dV_o \\ - \int_{\mathbf{B}_o} \left(\overset{\circ}{\mathbf{P}} \mathbf{L} \beta^T \right) \cdot \nabla_X \tilde{\boldsymbol{\eta}} dV_o = \\ \int_{\Gamma} \left\{ \overset{\circ}{\boldsymbol{\lambda}} - \left[\overset{\circ}{\mathbf{L}} \beta \cdot (\mathbf{N} \otimes \mathbf{N}) \right] \boldsymbol{\lambda} \right\} \cdot \tilde{\boldsymbol{\eta}} dA_o \end{aligned} \quad (23)$$

where $\tilde{\boldsymbol{\eta}}$ is a kinematically admissible sensitivity deformation field expressed over the reference configuration \mathbf{B}_o . The primary unknown of equation (23) is the design differential $\overset{\circ}{\mathbf{x}} = \overset{\circ}{\mathbf{x}}(\mathbf{Y}, t; \beta, \Delta \beta)$. In order to obtain the final form of the variational sensitivity problem, the relationships between (a) $\overset{\circ}{\mathbf{F}}_r$ and $\overset{\circ}{\mathbf{x}}$ (b) $\overset{\circ}{\mathbf{P}}$ and $\overset{\circ}{\mathbf{x}}$ (c) $\overset{\circ}{\boldsymbol{\lambda}}$ and $\overset{\circ}{\mathbf{x}}$ need to be developed. The relationship between $\overset{\circ}{\mathbf{F}}_r$ and $\overset{\circ}{\mathbf{x}}$ is purely kinematic and is given as follows (Fig. 7):

$$\overset{\circ}{\mathbf{F}}_r = \overline{\nabla_X \overset{\circ}{\mathbf{x}}} = \nabla_X \overset{\circ}{\mathbf{x}} - \mathbf{F}_r \mathbf{L} \beta \quad (24)$$

The relationship between $\overset{\circ}{\mathbf{P}}$ and $\overset{\circ}{\mathbf{F}}_r$ is obtained from the sensitivity constitutive problem and takes the form:

$$\overset{\circ}{\mathbf{P}} = \mathcal{A} [\overset{\circ}{\mathbf{F}}_r] + \mathcal{B} \quad (25)$$

where \mathcal{A} is a fourth order operator and \mathcal{B} a second order constant. The relationship between $\overset{\circ}{\boldsymbol{\lambda}}$ and $\overset{\circ}{\mathbf{x}}$ is obtained from the sensitivity contact problem as:

$$\overset{\circ}{\boldsymbol{\lambda}} = \mathbf{C} [\overset{\circ}{\mathbf{x}}] + \mathbf{d} \quad (26)$$

where \mathbf{C} is a second order tensor and \mathbf{d} a vector.

In the case where the design sensitivity analysis is performed to study the effects of variations in the parameter β_X (Fig. 6), a value of $\mathbf{L} \beta = \mathbf{0}$ is used and the driving force for the sensitivity problem are variations in the boundary conditions.

Consistent with the direct deformation analysis where an assumed (discrete) representation of the deformation gradient \mathbf{F}_r was used in the FE solution of the weak form, a sensitivity analysis is developed for the FE solution of the assumed strain \mathbf{F} -bar method. Let us denote the terms in the left-hand side of the sensitivity weak form in equation (23) by \mathcal{S}^{int} . The assumed strain sensitivity analysis involves the modification of the term \mathcal{S}^{int} in the FE representation of the sensitivity weak form. In the \mathbf{F} -bar method, only the constitutive response is modified. Thus $\overset{\circ}{\mathbf{P}} \equiv \overset{\circ}{\mathbf{P}}(\overset{\circ}{\mathbf{F}}_h^{ave})$ takes the form :

$$\overset{\circ}{\mathbf{P}} = \mathcal{A}[\overset{\circ}{\mathbf{F}}_h^{ave}] + \mathcal{B} \quad (27)$$

The assumed (discrete) sensitivity deformation gradient is obtained by the design differentiation of the volumetric-deviatoric decomposition introduced in equation (11) (Fig. 5):

$$\begin{aligned} \overset{\circ}{\mathbf{F}}_h^{ave} &= \epsilon \overset{\circ}{\mathbf{F}}_h + (1 - \epsilon) \overset{\circ}{\bar{\mathbf{F}}}_h \\ \overset{\circ}{\bar{\mathbf{F}}}_h &= \overset{\circ}{\bar{\mathbf{F}}}_h^{vol} \mathbf{F}_h^{dev} + \bar{\mathbf{F}}_h^{vol} \overset{\circ}{\mathbf{F}}_h^{dev} \\ \overset{\circ}{\bar{\mathbf{F}}}_h^{vol} &= \frac{\mathbf{I}}{3} \bar{J}_h^{-\frac{2}{3}} \left[\sum_{a=1}^{NINT} J_{ha}(\bar{\xi}_a) \text{tr}[\overset{\circ}{\mathbf{F}}_h(\bar{\xi}_a) \mathbf{F}_h^{-1}(\bar{\xi}_a)] \bar{N}_a \right] \\ \overset{\circ}{\mathbf{F}}_h^{dev} &= J_h^{-\frac{1}{3}} \overset{\circ}{\mathbf{F}}_h - \frac{1}{3} J_h^{-\frac{1}{3}} \mathbf{F}_h \text{tr}[\overset{\circ}{\mathbf{F}}_h \mathbf{F}_h^{-1}] \end{aligned} \quad (28)$$

Using the expressions given above, the assumed sensitivity deformation gradient which is used in the FE representation of the sensitivity weak form is given as follows:

$$\begin{aligned} \overset{\circ}{\mathbf{F}}_h^{ave} &= \left\{ \epsilon \overset{\circ}{\mathbf{F}}_h + (1 - \epsilon) \left[\frac{\bar{J}_h}{J} \right]^{\frac{1}{3}} \overset{\circ}{\bar{\mathbf{F}}}_h \right\} + \\ &\frac{1 - \epsilon}{3} \left[\sum_{a=1}^{NINT} J_{ha}(\bar{\xi}_a) \text{tr}[\overset{\circ}{\bar{\mathbf{F}}}_h(\bar{\xi}_a) \mathbf{F}_h^{-1}(\bar{\xi}_a)] \bar{N}_a \right] \bar{J}_h^{-1} \bar{\mathbf{F}}_h - \\ &\frac{1 - \epsilon}{3} \left\{ \text{tr}[\overset{\circ}{\mathbf{F}}_h \mathbf{F}_h^{-1}] \bar{\mathbf{F}}_h \right\} \end{aligned}$$

The term in the first paranthesis has the identical form that relates \mathbf{F}_h^{ave} and \mathbf{F}_h in the direct deformation problem. The latter terms result due to the fact that the assumed material gradient relationship depends on the current state of deformation and has to be linearized as well. To complete the analysis, the kinematic relationship between $\overset{\circ}{\bar{\mathbf{F}}}_h^{ave}$ and $\overset{\circ}{\mathbf{x}}_h$ needs to be developed. This is obtained by using equation (24) in the expressions for $\overset{\circ}{\mathbf{F}}_h$ and $\overset{\circ}{\bar{\mathbf{F}}}_h(\bar{\xi}_a)$:

$$\overset{\circ}{\mathbf{F}}_h = \nabla_X \overset{\circ}{\mathbf{x}}_h - \mathbf{F}_h \mathbf{L}$$

$$\overset{\circ}{\bar{\mathbf{F}}}_h(\bar{\xi}_a) = \nabla_X \overset{\circ}{\mathbf{x}}_h(\bar{\xi}_a) - \mathbf{F}_h(\bar{\xi}_a) \mathbf{L}(\bar{\xi}_a) \quad (29)$$

The modified term \mathcal{S}^{int} in the finite element representation is given as: $\mathcal{S}_h^{int} \equiv$

$$\begin{aligned} \sum_e \int_{\Omega_e} \left\{ \overset{\circ}{\mathbf{P}}(\overset{\circ}{\mathbf{F}}_h^{ave}) - [\mathbf{P}(\mathbf{F}_h^{ave}) \mathbf{L}^T] \right\} \cdot \nabla_X \tilde{\mathbf{q}}_h dV_o - \\ \int_{\Omega_e} \left(\mathbf{P}(\mathbf{F}_h^{ave}) [\nabla_X \cdot \mathbf{L}^T] \right) \cdot \tilde{\mathbf{q}}_h dV_o \end{aligned}$$

SENSITIVITY CONSTITUTIVE PROBLEM As part of this sub-problem, the relationship between $\overset{\circ}{\mathbf{P}}$ and $\overset{\circ}{\mathbf{F}}_r$ at time t_{n+1} as used in the solution of the sensitivity deformation problem is computed. The solution of the direct deformation problem is known at time t_{n+1} . Due to the non linear material response, the constitutive sensitivity problem is history dependent and the solution of the sensitivity problem at time t_n is assumed known. Thus, the solution of the sensitivity constitutive sub-problem is advanced within the incremental solution scheme by integrating the evolution equations for the sensitivity of the plastic deformation gradient \mathbf{F}^p and the evolution equation for the sensitivity of state variable s [1],[2].

The evolution of the sensitivity of the plastic deformation gradient \mathbf{F}^p is obtained by the design differentiation of the flow rule as:

$$\frac{\partial \overset{\circ}{\mathbf{F}}^p}{\partial t} = \bar{\mathbf{D}}^p \overset{\circ}{\mathbf{F}}^p + \bar{\mathbf{D}}^p \mathbf{F}^p \quad (30)$$

The evolution equation for $\overset{\circ}{s}$ is obtained by taking the direct variation of the state variable evolution (equation (4)) i.e.

$$\frac{\partial \overset{\circ}{s}}{\partial t} = g_{\bar{s}} \overset{\circ}{\bar{s}} + g_s \overset{\circ}{s} \quad (31)$$

Time integration of these sensitivity constitutive equations is performed using the same Euler-backward temporal integrator which was used for the corresponding equations in the direct constitutive problem. The relationship between the sensitivity of the deformation gradient \mathbf{F}_r and the sensitivity of the elastic deformation gradient \mathbf{F}^e is obtained using :

$$\overset{\circ}{\mathbf{F}} = \overset{\circ}{\mathbf{F}}^e \mathbf{F}^p + \mathbf{F}^e \overset{\circ}{\mathbf{F}}^p = \overset{\circ}{\mathbf{F}}_r \mathbf{F}_o + \mathbf{F}_r \overset{\circ}{\mathbf{F}}_o \quad (32)$$

The relationship between $\overset{\circ}{\mathbf{T}}$ and $\overset{\circ}{\mathbf{F}}^e$ is obtained using the sensitivity of the hyperelastic constitutive law (equation (4)). The relationship between $\overset{\circ}{\mathbf{F}}_{n+1}^p$ and $\overset{\circ}{\mathbf{F}}_{n+1}^e$ is obtained after the temporal integration of the evolution equations developed in equations (30) and

(31). Therefore, one can finally obtain a relationship between $\overset{\circ}{\mathbf{T}}$ and $\overset{\circ}{\mathbf{F}}_r$ (using equation (32)). Note that the relationship between $\overset{\circ}{\mathbf{P}}$ and $\overset{\circ}{\mathbf{F}}_r$ is known, if the relationship between $\overset{\circ}{\mathbf{T}}$ and $\overset{\circ}{\mathbf{F}}_r$ is computed. (by consideration of the relation between the two stress measures in equation (3)).

The sensitivity constitutive sub-problem is essentially identical for studying variations with respect to β_X or β_Y . The main feature which contrasts these is in the interpretation of $\overset{\circ}{\mathbf{F}}_r$, which in the case of variation with respect to β_Y is clearly dependent on $\mathbf{L}\beta$. Consider the design sensitivity analysis to study the effects of variation in the parameter β_Y . Let $Q = (\mathbf{F}^p, s)$ represent the collection of plastic deformation gradient and the isotropic resistance to deformation. As a result of the deformation process history defined by the design parameters β_Y , the intermediate preform is characterized by a specific distribution $\overset{\circ}{Q}$ which affects the initial conditions of the sensitivity constitutive problem.

The sensitivity deformation problem presented here can also be used in the analysis of the sensitivity of the unloading process at the end of the forming stage. In this case, we need to consider the sensitivity of a finite deformation elasto-static problem. Thus the sensitivity constitutive problem presented above is modified and the material deformation behaviour treated as elastic in the unloading phase. In particular the relationship between $\overset{\circ}{\mathbf{P}}$ and $\overset{\circ}{\mathbf{F}}_r$ is determined by an elastic constitutive law with frozen sensitivities of state during the unloading phase $\overset{\circ}{\mathbf{F}}_u = \overset{\circ}{\mathbf{F}}^p$ and $\overset{\circ}{s}_u = \overset{\circ}{s}$. The duration inbetween forming stages is characterized by the evolution of the sensitivity of the inelastic internal variable (recovery phase).

SENSITIVITY CONTACT PROBLEM As part of this sub-problem, the relationship between the sensitivity of the contact traction $\overset{\circ}{\boldsymbol{\lambda}}$ and $\overset{\circ}{\mathbf{x}}$ at time t_{n+1} as used in the solution of the sensitivity deformation problem is computed. The sensitivity of a function $f = f(\mathbf{x})$, denoted by $\overline{[f(\mathbf{x})]}$ generally consists of two parts, the first part, $\overset{\circ}{f}$, denotes the contribution due to changes in the function f with \mathbf{x} constant and the second part, $\nabla f \overset{\circ}{\mathbf{x}}$, denotes the contribution due to changes in the variable \mathbf{x} with f constant:

$$\overline{[f(\mathbf{x})]} = \overset{\circ}{f} + \nabla f \overset{\circ}{\mathbf{x}} \quad (33)$$

In the case where $\beta = \beta_X$ represents the die shape, explicit changes in the die shape are represented by $\overset{\circ}{\mathbf{y}}\beta$ ($\xi = \mathbf{y}_{(\beta+\Delta\beta)}(\xi) - \mathbf{y}_\beta(\xi)$) and result in explicit changes

in the normal and tangential vectors to the die ($\overset{\circ}{\boldsymbol{\nu}}_\beta, \overset{\circ}{\mathbf{r}}_\beta$). For computing the sensitivity with respect to all other parameters β , we have $\overset{\circ}{\mathbf{y}}\beta = \mathbf{0}$.

As a result of the non-smooth nature of the contact/friction conditions, the following regularizing assumptions are made in the computation of the sensitivities, to allow for differentiability: *Transition from stick to slip condition and/or from contact to non-contact (or vice versa) does not occur at a material point as a result of a perturbation to the design parameters*[1],[2].

Consideration of the strong form of the normal contact constraints in the direct deformation problem yields for points in contact $g(\mathbf{x}_{n+1}) = 0$ and $\lambda_N > 0$. Thus, the normal contact sensitivity constraint is obtained as $\overline{g(\mathbf{x}_{n+1})} = 0$ and $\overset{\circ}{\lambda}_N \in \Re$. The following penalty form is used to enforce this constraint:

$$\overset{\circ}{\lambda}_N = \overset{\circ}{\lambda}_{N_n} + \epsilon_N \overline{g(\mathbf{x}_{n+1})} \quad (34)$$

where $\overset{\circ}{\lambda}_{N_n}$ is the sensitivity of the normal traction component at the beginning of the time integration step. Consideration of the tangential contact constraints yields that for points in sticking contact, $\overset{\circ}{\xi} = 0$. The corresponding sensitivity constraint takes the form: $\overline{\overset{\circ}{\xi}} = \overset{\circ}{\xi} = 0$. The following penalty formulation of the sticking sensitivity constraint is introduced:

$$\overset{\circ}{\xi} = \frac{1}{\epsilon_T} \overset{\circ}{\lambda}_T \quad (35)$$

Integration of this equation results in the following:

$$\overset{\circ}{\lambda}_T = \overset{\circ}{\lambda}_{T_n} + \epsilon_T \left(\overset{\circ}{\xi} - \overset{\circ}{\xi}_n \right) \quad (36)$$

where $\overset{\circ}{\lambda}_{T_n}$ is the sensitivity of the tangential traction component at the beginning of the time integration step. In the case of slip, λ_T is well defined by the Coulomb friction law as:

$$\overset{\circ}{\lambda}_T = \overline{\left(\mu \lambda_N \frac{1}{\|\boldsymbol{\tau}_1\|} \right)} \quad (37)$$

The sensitivity of the contact traction vector is given as:

$$\overset{\circ}{\boldsymbol{\lambda}} = \overline{\lambda_N \boldsymbol{\nu}(\bar{\mathbf{y}})} - \overline{\lambda_T \boldsymbol{\tau}_1(\bar{\mathbf{y}})} \quad (38)$$

and can be shown to take the form:

$$\overset{\circ}{\boldsymbol{\lambda}} = \overset{\circ}{g} \boldsymbol{\gamma}_1 + \overset{\circ}{\xi} \boldsymbol{\gamma}_2 + \boldsymbol{\gamma}_3 \quad (39)$$

where γ_i are known vectors computed using the developments described above. It can be shown that, $\dot{\xi}$ which represents the sensitivity of the amount of inelastic slip is related to $\dot{\mathbf{x}}$. This linear relationship between $\dot{\xi}$ and $\dot{\mathbf{x}}$ can be developed by consideration of the fact that the closest point $\bar{\mathbf{y}}$ on the die to a point \mathbf{x} is the projection of the point \mathbf{x} on to the die. The linear relationship between the sensitivity of the gap function $\overline{g(\mathbf{x})}$ and $\dot{\mathbf{x}}$ can be obtained by the design differentiation of the gap function.

DESIGN EXAMPLES Two representative examples for metal forming design are presented here. The material chosen for the workpiece is 1100-Al at a temperature of 673 K [9]. The \mathbf{F} -bar method with a stabilization factor $\epsilon = 10^{-03}$ and four noded quadrilateral elements is used in the simulation. Additional details on the direct problem can be found in [10]. B-splines are used for the representation of the dies and preforms with the control points of the curve used as design variables.

Preform net-shape design in a single stage forging process to minimize the upsetting force: Design a preform shape of height $2H$ that encompasses (overlaps) a prescribed shape of height $2h$ in a single stage upsetting process and requires the minimal upsetting force during the process. Fig. 8 presents a schematic of the optimization problem.

A friction coefficient of 0.4 is assumed at the die-workpiece interface. The forging force is here taken as the maximum force in the axial direction during the process. This force at the final stroke expressed in terms of the contact tractions as follows:

$$f(\beta) = \int_{\Gamma} \lambda \cdot \mathbf{e}_z dA_o \quad (40)$$

where $\Gamma \subset \mathbf{B}_o$. While computing the shape sensitivity of the force, it is important to note that the initial area (the subset of Γ) that is in contact with the die changes with the preform. Therefore:

$$\dot{f} = \int_{\Gamma} \dot{\lambda} \cdot \mathbf{e}_z dA_o + \int_{\Gamma} \lambda \cdot \mathbf{e}_z \frac{\dot{dA}_o}{d\beta} \quad (41)$$

Differentiation of the term $\frac{\dot{dA}_o}{d\beta}$ can be shown to be related to \mathbf{L}_β . The free surface R_β is assumed to be parametrized using 6 basis functions as in Example 4 of [2]. The inequality constraint on the shape of the final product is expressed in the form of an overlap equality constraint as follows:

$$\begin{aligned} h(\beta) &= \int_{\Gamma_F} \langle g(\beta) \rangle d\Gamma_F \\ g(\beta) &= r_p - x_1(\beta) \end{aligned} \quad (42)$$

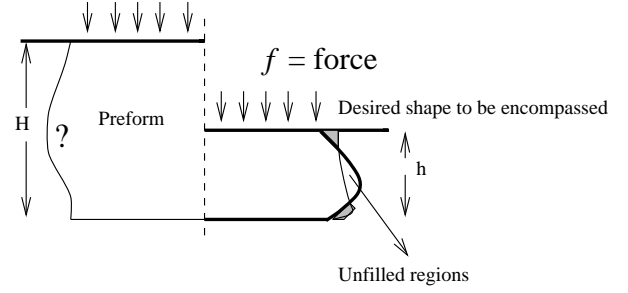


FIGURE 8: Schematic of a $\frac{1}{4}$ geometry model of the preform shape design problem which minimizes the upsetting force in an upset forging process ($H = 1.0 \text{ mm}$, $h = 1.0 \text{ mm}$) (Example 1).

where r_p is the prescribed shape, $\langle \cdot \rangle$ is the Macauley bracket and Γ_F is the free surface. The prescribed shape r_p is a cubic function of the height from the equatorial plane of the final product z :

$$r_p(z) = a z^3 + b z^2 + c z + d \quad (43)$$

and the constants are specified as $a = 1.0$, $b = -3.0$, $c = 2.25$, and $d = 1.0$. A penalty method is used to convert the constrained optimization problem to an unconstrained one. The penalty function chosen is given as:

$$\min P(\beta) = f(\beta) + \omega h(\beta) \quad (44)$$

and the penalty parameter is taken as $\omega = 10^{03}$. The steepest-descent method is used to solve the unconstrained minimization problem defined by the penalty function. Figure 9 represents the variation of the objective function during iterations. Results indicate that optimal preform is obtained using 13 iterations including 4 line searches. Figure 10 represents the undeformed and deformed configurations for the initial, intermediate and the optimal preforms as well as the prescribed final shape to be encompassed. It is noted that the initial preform corresponding to that of right cylinder of radius 1.00 mm required a force of 78.21 N, but represents an infeasible solution. The optimal preform required a force of 76.65 N. After feasibility was satisfied in the optimization iterations (corresponding to iteration 3), a decrease in the upsetting force of 18.23% was observed. The importance being able to model such a net-shape optimization application is realized in the shop floor where tools and equipment required to apply the forging force are often subject to limitations.

Preform die shape design in a two-stage forging sequence to minimize barreling: Design the die shape in the pre-forming stage, so that the forging sequence comprised of a subsequent finishing stage with a flat die yields a

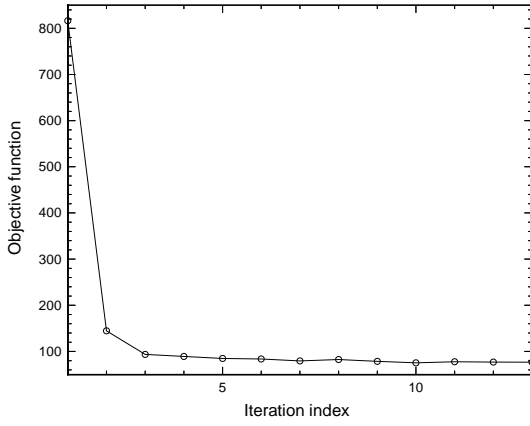


FIGURE 9: Variation of the modified objective function versus the optimization iteration index (Example 1).

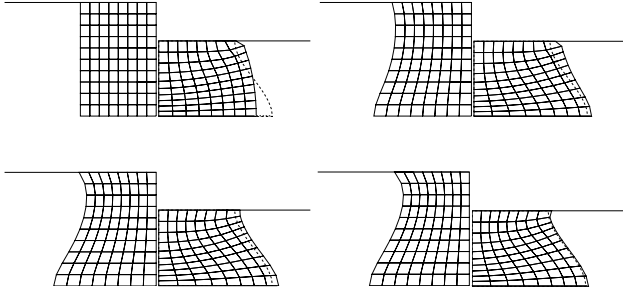


FIGURE 10: The initial, intermediate (iterations 4 and 7) and optimal die shapes of the upset forging process minimizing the upsetting force (Example 1).

circular cylinder of radius r and height $2h$ (i.e. a final product of given height with no barreling). The virgin product has a specified radius R and height $2H$. Fig. 11 provides a schematic of this optimization problem.

A friction coefficient of 0.20 was assumed at the die-workpiece interface. The initial preform die shape was chosen to correspond to that of a flat die and the die strokes for the two stages are specified. The preform die shape is represented using a 6th order Bézier curve with 5 independent variables.

$$\begin{aligned} r(\alpha) &= 1.5(1 - \alpha), \quad \alpha \in [0.0, 1.0] \\ z_{\beta}(\alpha) &= \sum_{i=1}^6 \beta_i \phi_i(\alpha) \end{aligned} \quad (45)$$

The height of the die at $r = 0$ was specified and as a

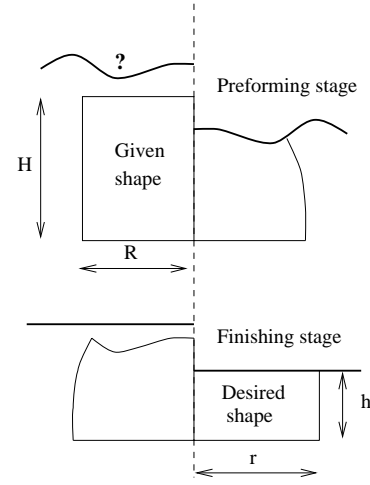


FIGURE 11: Schematic of a $\frac{1}{4}$ geometry model of the two-stage design problem which minimizes barreling in an upset forging process ($H = 1.0 \text{ mm}$, $h = 0.5 \text{ mm}$, $R = 1.00 \text{ mm}$, $r = 1.4142 \text{ mm}$) (Example 2).

result of the axisymmetry of the problem, the die shape was assumed to have a zero slope at $r = 0$. This lead to the following basis functions:

$$\begin{aligned} \phi_1 &= (1.0 - \alpha)^6 \\ \phi_2 &= 6.0(1.0 - \alpha)^5 \alpha \\ \phi_3 &= 15.0 (1.0 - \alpha)^4 \alpha^2 \\ \phi_4 &= 20.0 (1.0 - \alpha)^3 \alpha^3 \\ \phi_5 &= 15.0 (1.0 - \alpha)^2 \alpha^4 \\ \phi_6 &= (6.0 - 5\alpha)\alpha^5 \end{aligned}$$

and the variable ($\beta_6 = 1.3$) was chosen which fixed the height and the slope of the die at $r = 0$. The finite dimensional optimization problem can be now posed as:

$$\min f(\beta) = \int_{\Gamma_F} (x_1(\beta) - r)^2 d\Gamma_F + \int_{\Gamma_T} (x_2(\beta) - h)^2 d\Gamma_T$$

where $\beta = (\beta_1, \dots, \beta_5)$ and Γ_F , Γ_T refer to the free surface and top surface of the final product, respectively.

Since we consider a $\frac{1}{4}$ geometry model in the present simulation, the modeling of the unloading phase which necessitates removal of *one* of the dies from contact with the workpiece is not possible. Therefore, the residual stresses are considered negligible (zero) before the start of the second stage. From Figure 13, it is clear that with the initial flat preform die shape, there is a significant amount of barreling in the final product. The steepest-descent method is used to solve the minimization problem. Figure 12 represents the variation of the objective

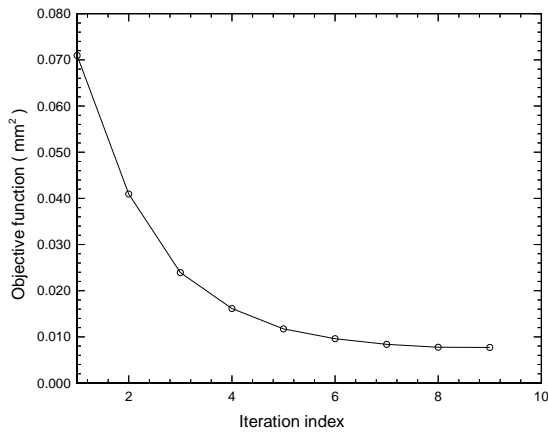


FIGURE 12: Variation of the objective function which quantifies the amount of barreling in the final product versus the optimization iteration index (Example 2).

function during iterations. Results indicate that the near-optimal preform is essentially obtained using 9 iterations. Note that although the barreling has been significantly reduced, it has not been completely eliminated. Similar observations were also made for higher coefficients of friction (e.g. 0.4). Figure 13 represents the initial, intermediate and final products for the preforming and finishing stages of the forming sequence. Figure 14 represents the distribution of equivalent plastic strain and the state variable in the final product corresponding to the optimal preform die shape. The values represented here are the result of processing in both the preforming and finishing stages.

ACKNOWLEDGEMENTS The work presented here was funded by grants from (a) NSF (DMII-9522613), (b) Materials and Manufacturing Directorate of the Air Force Research Laboratory at Wright-Patterson Air Force Base (Dr. Garth Frazier, Program Manager) (c) Alcoa Laboratories (Dr. Paul Wang, Program manager). The computing for this project was supported by the Cornell Theory Center. The simulator was developed using the object oriented FEM environment of *diffpack*. The academic license for using the various libraries of *diffpack* is appreciated.

REFERENCES

1. N. Zabaraz, Y. Bao, A. Srikanth and W. G. Frazier, A continuum Lagrangian sensitivity analysis for metal forming processes with applications to die design problems, *Int. j. numer. methods engr.*, in press.
2. A. Srikanth and N. Zabaraz, Shape optimization and

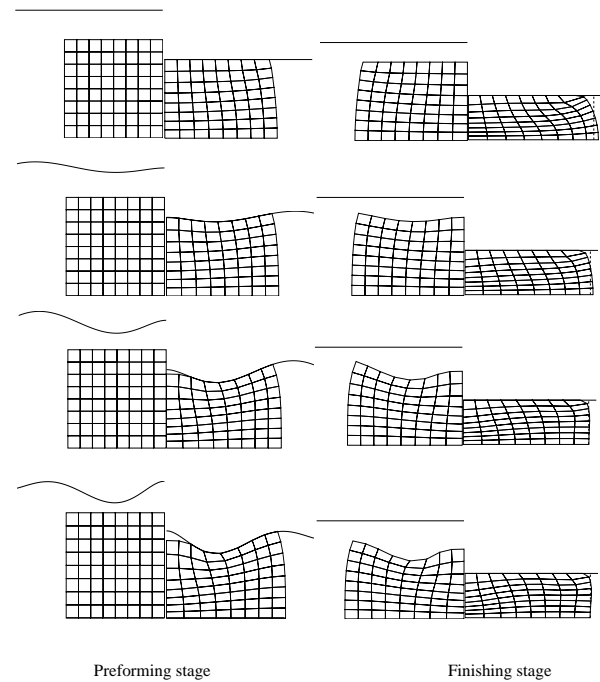


FIGURE 13: The preforming and finishing stages of the initial, intermediate (iterations 3 and 6) and optimal die shapes of the two stage forging process minimizing barreling in the final product (Example 2).

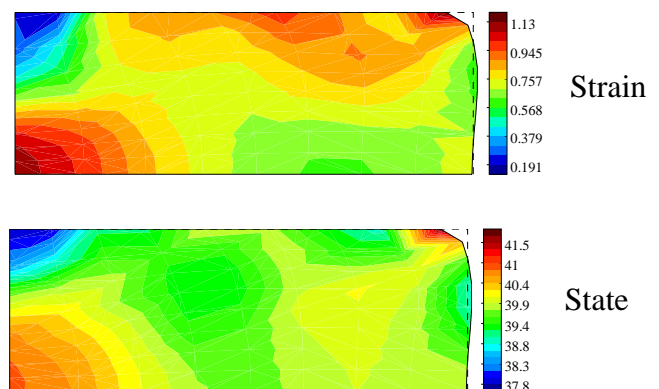


FIGURE 14: The variation of equivalent plastic strain and the scalar state variable which represents the isotropic resistance to deformation, in the final product corresponding to the optimal preform die shape (Example 2).

- perform design in metal forming processes, *Comput. methods appl. mech. engr.*, in press.
3. N. Zabaras and A. Srikanth, Using objects to model finite deformation plasticity, *Engineering with computers*, Vol. 15(1) (1999) 37-60.
 4. G. Weber and L. Anand, Finite deformation constitutive equations and a time integration procedure for isotropic, hyperelastic-viscoplastic solids, *Comp. methods appl. mech. engr.*, Vol. 79, (1990) 173-202.
 5. T. A. Laursen and J. C. Simo, On the formulation and numerical treatment of finite deformation frictional contact problems, *Nonlinear computational mechanics- State of the art*, (eds.) P. Wriggers and W. Wager, Springer Verlag, Berlin, (1991) 716-736.
 6. B. Moran, M. Ortiz and C. F. Shih, Formulation of implicit finite element methods for multiplicative finite deformation plasticity, *Int. j. numer. methods engr.*, Vol. 29, (1990) 483-514.
 7. E. A. de Souza Neto, D. Perić, M. Dutko and D. R. J. Owen, Design of simple low order finite elements for large strain analysis of nearly incompressible solids, *Int. j. solids structures*, Vol. 33, (1996) 3277-3296.
 8. P. Hansbo, A new approach to quadrature for finite elements incorporating hourglass control as a special case, *Comp. methods appl. mech. engr.*, Vol. 158, (1998) 301-309.
 9. S. B. Brown, K. H. Kim and L. Anand, An internal variable constitutive model for hot working of metals, *Int. j. plasticity*, Vol. 5, (1989) 95-130.
 10. A. Srikanth and N. Zabaras, A computational model for the finite element analysis of thermoplasticity with ductile damage at finite strains, *Int. j. numer. methods engr.*, Vol. 45, (1999) 1569-1605.